2006

Cycle-Resolved Velocity Measurements Within a Screw Compressor

J. M. Nouri
The City University

D. Gueratto
The City University

Nikola Stosic
The City University

Ahmed Kovacevic
The City University

C. Arcoumanis
The City University

CYCLE-RESOLVED VELOCITY MEASUREMENTS WITHIN A SCREW COMPRESSOR

J. M. Nouri, D. Guerrato, N. Stosic, A. Kovacevic and C Arcoumanis
School of Engineering and Mathematical Sciences
The City University, London EC1V OHB, U.K.
Tel +44 20 7040 8925, Fax +44 7040 8566, e-mail: n.stosic@city.ac.uk

ABSTRACT

This paper presents the initial experimental results of a long term programme, the ultimate aim of which is to be able to produce software for the design of twin screw compressors and expanders in which full account is taken of 3-D flow and fluid-solid interactive effects on performance. Software for this purpose, based on CFD methods has already been developed but requires reliable measurements of velocity and pressure fields within the machine, throughout its operating cycle, in order to be validated. Hitherto, no record of any such measurements has been reported. Measurements of the phase-averaged mean velocity components and the corresponding turbulence fluctuations within the compressor working chamber will therefore be evaluated by means of Laser Doppler Velocimetry (LDV), at various cross sections, including inlet and exit, under both steady and transient flow conditions. A standard air compressor test rig has been adapted for this purpose and fitted with an oil injected screw compressor, modified by fitting it with a transparent window near the discharge port to allow the application of various laser measuring techniques. As the initial phase of the measurements, the axial mean and root mean square velocities were measured in the compressor inside the compression chamber at rotational speeds of up to 1,000 rpm. The results so far, have confirmed the usefulness of the LDV technique as a means of measuring the flow inside the compressor working chamber and showed that an angular resolution of 2° is small enough to fully describe the flow inside the chamber. It was also found that flow variation between successive working chambers within the male rotor was small and that the variation of the axial mean velocity and turbulence velocity fluctuation within the working chamber could be identified.

Keywords: Screw Compressor, Laser Doppler Velocimetry, Computational Fluid Dynamics

1. INTRODUCTION

Screw compressors are widely used in industry. In particular, they have replaced the traditional reciprocating compressor over a large range of operating conditions in air compression and refrigerant compression systems, while, more recently, their use as superchargers in the automotive industry is increasing. To maintain their advantage, there is a continuing need to improve their design in order to reduce energy consumption, noise generation and manufacturing costs.

A screw compressor comprises a pair of rotors contained within a casing in which their meshing lobes form a series of working chambers within which the compression process takes place. As the rotors revolve, the gas, to be compressed, flows into the space between the rotor lobes and the suction port. Further rotation leads to cut-off of the suction port so that the trapped volume is pushed forward both axially and circumferentially towards the discharge port by the screw rotor motion. This is accompanied by reduction of the trapped volume in each passage, which causes the pressure to increase. This process continues until the working volume between the rotors is exposed to the discharge port through which the high pressure gas is expelled. The fluid flow through such compressors is therefore highly unsteady and, although it is analogous to that in reciprocating machines, is far more complex, due to the rotational motion of the working chamber, which changes both in size and shape, and leads to significant 3-D effects. The compressor design can only be optimized if the fluid flow through the suction and discharge ports, the working chambers and the clearance gaps within them, can be predicted accurately. Currently, most designs are carried out using one-dimensional flow models. These are not adequate for the design of the ports nor do they allow for local variations within the working chamber due to distortion induced by the pressure and temperature changes.

Efforts have therefore been made to use 3-D analysis to quantify these effects, where they are significant, by means of Computational Fluid Dynamics (CFD) and Computational Continuum Mechanics (CCM) procedures. However, to date, no record of unsteady gas velocity measurements in the screw compressor working volume and its suction and discharge chambers, during the operating cycle, have been reported to validate such analyses.

The potential benefits to be derived from the ability to optimise port design and to make the correct allowance for rotor and casing distortion, with the minimum amount of testing, are large, especially when applied to oil free machines, in which temperature changes are large, and if the analytical procedures used, result in decreased product development time.

With these aims in view, the material presented in this paper, describes the initial stages of a long term research project, attempting to measure the fluid mean velocity distribution and the corresponding turbulence fluctuations, at various cross-sections of the compressor working volume, within the interlobe space, at different phase angles, in sufficient detail to enable the flow through the whole working space to be estimated accurately. This will reveal how major features of the heat and fluid flow within the machine are affected by the rotor and lobe geometry. The investigation includes measurement of major integral properties of the compressor, including the suction and discharge pressures and temperatures, the flow delivery and torque/power by standard laboratory-type instruments. By this means, the test results will be compared with predicted values of the same properties derived from an existing CFD model (9-15). The hoped for result is thus to validate and further develop the CFD package, to a stage which will render it capable of improving the design of future screw compressors.

As described above, the flow in the compressor is complex, three dimensional and strongly time dependent with strong similarities to that in gasoline and diesel engine cylinders [1, 2], centrifugal pumps [3], turbochargers [4 - 6] and mixing reactors agitated by turbines [7]. This implies that the measuring instrumentation must be robust to withstand the unsteady aerodynamic forces, have high spatial and temporal resolution and, most importantly, must not disturb the flow. Only point optical diagnostics like Laser Doppler Velocimetry (LDV) can fulfil these requirements, as described in these earlier studies (1-7). The method of investigation proposed for the screw compressor studies was therefore to determine the fluid velocity and turbulence fluctuations at a range of pre-selected measurement points using an existing Dual beam Laser-Doppler Velocimeter. These results were to be complemented by flow field measurements using high speed particle image velocimetry (PIV). The main advantage of PIV is its ability to characterize two-dimensional, rather than point, instantaneous flow fields, thus revealing 2-D angle-phased flow structures.

The main objective of the present work was to try out the LDV method inside a compressor and to identify any problems related to its use for this application. A dual beam LDV system was used to obtain both the angle-resolved axial mean and the turbulence properties of the flow, at a location near the discharge port of the compressor in the interlobe region, at different radial positions inside the working chamber. A transparent window made of acrylic plexiglass was installed on the high pressure side that was large enough to allow near backscatter light collection. The internal profile of the window was exactly the same as that of the rotor's casing, as shown in Fig 2(c), in order to minimise flow disturbance and preserve the integrity of flow motion. Its effect on the flow was only on the roughness of the wall which is smoother in the area of the window.

2. FLOW CONFIGURATION AND MEASURING INSTRUMENTS

The test measurements were made on an air compressor test rig that meets Pneurop/Cagi PN2CPTC1 requirements for screw compressor acceptance tests that was modified to accommodate the new optical compressor, the transmitting and collecting optics and their traverses**.** The compressor was tested according to ISO 1217 and its delivery flow was measured following ISO 5716. High accuracy test equipment was used for the measurement of all relevant parameters. All measurements were taken by transducers and both recorded and processed in a computerized data logger for real time presentation. The test rig layout is presented in Fig. 1. A 75 kW electrical motor with variable speed controlled by a frequency converter was used as a prime mover via a torque meter. Measured values were used to calculate compressor flow, power and specific power, while the oil injection rate was estimated by means of a heat balance.

A standard oil injected screw compressor was used For the LDV velocity measurements. The transparent window was machined from acrylic to the exact internal profile of the rotor case, as shown in Fig. 2(a), and was positioned on its high pressure side, near the discharge port, as shown in Fig. 2(b). After machining the internal and external surfaces of the window were polished to allow optical access. Angle-resolved axial velocity measurements were

performed along a radial plane inside the working chambers of the male rotor near the discharge port. Fig. 3 shows photographs of the working chamber geometry of the male and female rotors and the interrogation area, which is traversed by five working chambers, formed by the lobes of the male rotor, during one cycle. The radial plane along which the velocity measurements were made was 27º to the vertical at a distance 73 mm from the centre of the discharge port. The zero radial position coincides with the centre of the rotor, but the radial location at which the working chamber starts is at r=39.5 mm. The axial velocity component in the rotors is positive in the direction going from the suction port to the discharge port.

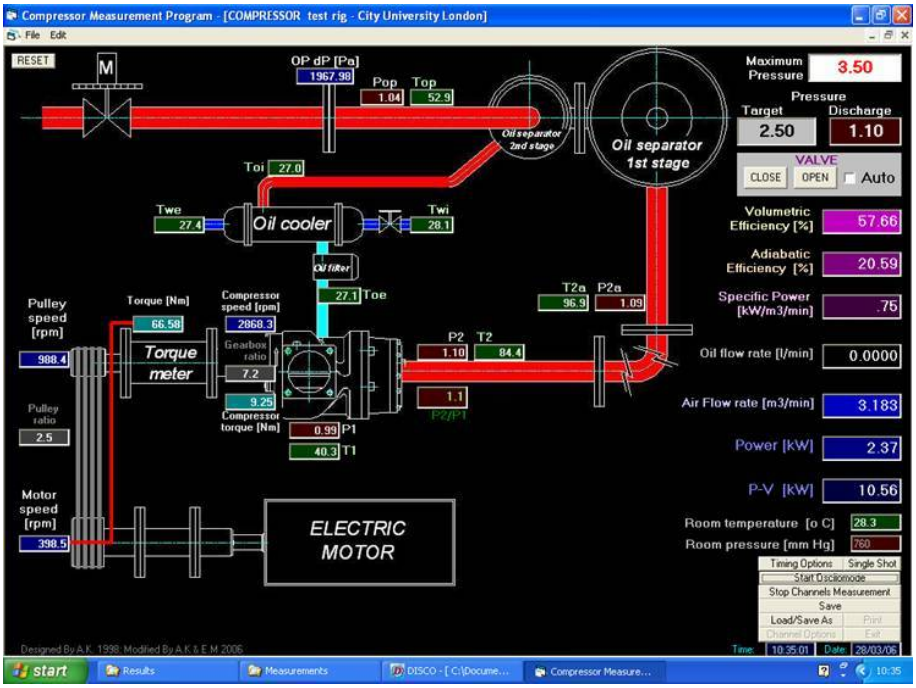

Figure 1 Layout of the compressor test rig

Under normal compressor operating conditions, oil is injected for cooling purposes. However, even at the lowest possible flow rate, the presence of the oil caused serious flooding inside the working chamber especially on the inner surface of the optical window, thus forming an unstable thick oil film. Under such condition no LDV or any other optical method is practical because the laser beams passing through this oil film will be distorted, causing uncertainties in the geometry of the measuring volume, especially at the crossing of the two beams. It was therefore decided to run the compressor at low speeds with no oil injection in order to obtain measurements. Over this speed range, the maximum air temperature was 60±3ºC for a speed of 1000 rpm, with a corresponding value of 55±3ºC at 750 rpm. In this way the true flow characteristics induced between the rotors and the casing by rotation of the rotors, in the region of the male rotor, could be evaluated.

The flow regime was identified by the Reynolds number, in which, V_p is the male rotor pitch radius tangential velocity, which was estimated to be 2.957 and 3.94 m/s at rotor speeds of 750 and 1000 rpm, respectively, and D_p is the male rotor pitch diameter, which is 81.8 mm. The blade's pitch velocity was derived from the rotor lead helix angle, which is 42.63 degrees. The calculated Reynolds number was found to be 13200 and 17100 for rotor speeds of 750 and 1000 rpm, respectively. The flows under these speeds could therefore be considered to be turbulent. The volumetric flow rates through the compressor were measured by an orifice plate installed in the exhaust pipe and were 0.842 m^3/min and 1.047 m^3/min for rotational speeds of 750 and 1000 rpm, respectively. For the LDV application it is essential to seed the flow so that the seeds, inside the measuring volume, can scatter light, from which their velocity can be obtained. The size of these particles/droplets should be small enough to ensure that all of them are following not only the mean flow but also the velocity fluctuations. For that reason a silicone oil atomiser that was purposely made for LDV measurements was used, which produced droplets of 1 to 2 μm diameter when spraying a low viscosity silicone oil of 5 cSt.

The laser Doppler velocimeter was operated in dual-beam near backscatter mode and comprised a 600 mW argon-ion laser, a diffraction-grating unit to divide the light beam into two and provide frequency shift, and collimating and focusing lenses to form the control volume. A fibre optic cable was used to direct the laser beam from the laser to the transmitting optics, and a mirror was used to direct the beams from transmitting optics into the compressor through the transparent window, as shown in Fig 2 (c). The collecting optics were positioned at aproximately 25° to the full backscatter position and comprised collimating and focusing lenses, a 100 μm pin hole and a photomultiplier equipped with an amplifier. The size of the pinhole forms the effective length of the measuring volume and its diameter and fringe spacing were calculated to be 79 μm and 4.33 μm, respectively. The signal from the photomultiplier was processed by a new TSI processor interfaced to a PC and led to angle-average values of the mean and rms velocities. In order to synchronise the velocity measurements with respect to the location of the rotor lobes, a shaft encoder that provides one pulse per revolution and 3600 train pulses, thus giving an angular resolution of 0.1°, was fixed to the end of driving shaft. Instantaneous velocity measurements were made over thousands of shaft rotations to provide a sufficient number of samples, which in the present study was set at 50,000.

(a) (b)

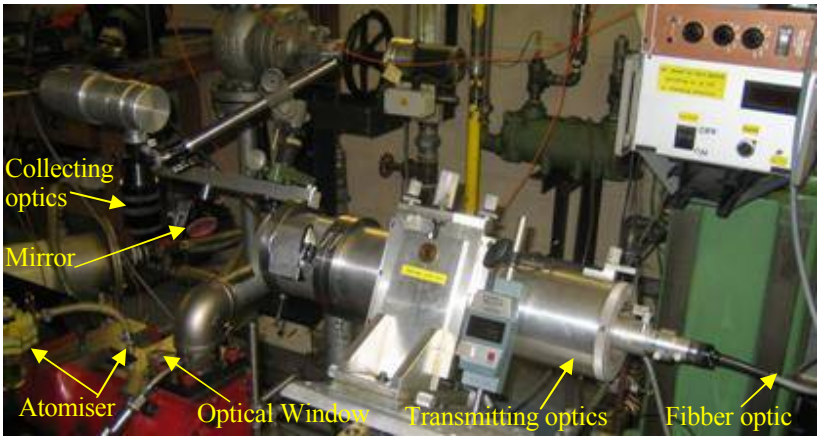

(c)

Figure 2 Optical compressor set up: (a) transparent window and its internal profile; (b) modified compressor with transparent window near the discharge; (c) LDV optical set up of transmitting and collecting optics.

A Matlab program was written to resolve the velocity, with respect to the rotor position, from the shaft angular position derived from the shaft encoder, in what are termed 'gated' measurements. This was done by collecting the sum of all the instantaneous velocities over a given time-window (2° of one revolution in this experiment) and then calculating the mean, U, and rms, u, values from the total. This method of gated measurements was effective since the data was collected continuously as the rotor turned and provided ensemble averages for every 2° over the entire 360° cycle in a time interval of up to 25 minutes. This gave more than 600 samples per time-window which yields statistical uncertainties of less than 1.6% and 5.5% for the ensemble mean and rms velocities respectively, based on

the assumption of a 95% confidence level and a velocity fluctuation of 20% of the mean value. A second program was written to calculate the location of the measuring volume in the compressor that included the refractive effects of the transparent window.

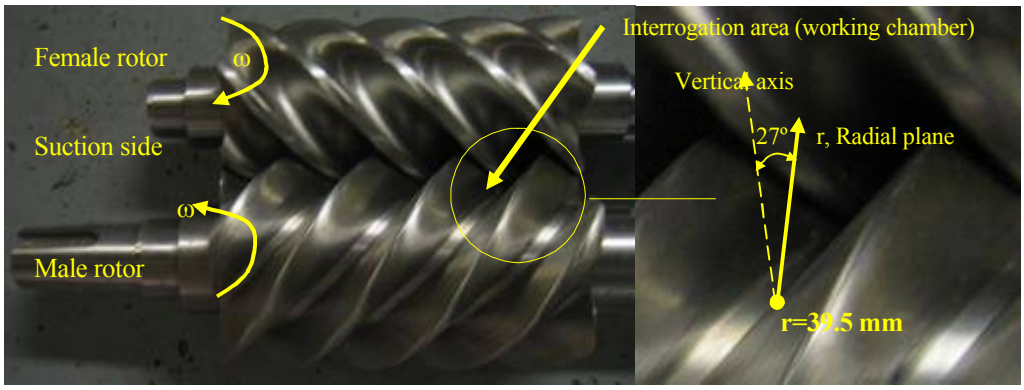

(a) (b)

Figure 3 Photographs of the male and female screw rotors with the enlarged working chamber (interrogation area) in the pressure side of the compressor near the discharge port.

3. TEST RESULTS AND DISCUSSION

The results of the axial mean and rms velocity estimates for the male rotor are presented in Figs 4 to 10 to quantify the following effects:

i) The effect of different resolving angles, shown in Fig 4

ii) The effect of flow variations in successive working chambers, as quantified in Figs 5 and 6.

iii) Axial flow characteristics at different radial locations, as described in Figs 7 to 10.

Note that in all the figures presented, the rotation of the rotor is anti-clockwise, viewed from the compressor suction side, with the region immediately behind the rotor lobe referred to as the trailing edge region and in front of the lobe as the leading edge region.

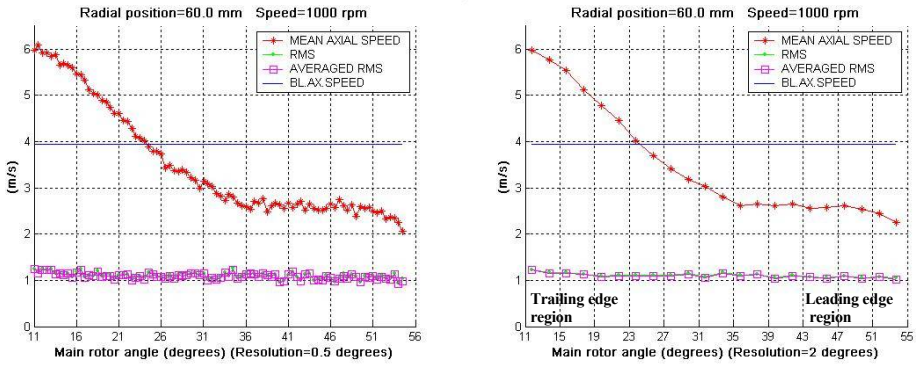

(a) (b)

Figure 4 Angular variation of axial mean and rms velocities across the working chamber for two angle-windows resolution of 0.5 and 2 degrees at a radial position of r=60 mm and at a rotational speed of 1000 rpm.

The mean and rms velocities resolved over angles of 0.5 and 2 degrees are presented in Fig 4. It clear that the mean flow obtained at both resolving angles leads to the same mean flow pattern, of an identical magnitude, while the overall fluctuation in the mean velocities is well within the experimental error. Similar behavior can be seen for the

turbulence velocity fluctuation variations with the same profiles. The only difference is the number of averaged values for 0.5° resolution which is four times higher than with 2° resolution. The results indicated that the 2° resolved angle-widows give the same mean and turbulence flow structures to that for 0.5°, and thus an angle-window of 2° was chosen to present the mean and rms velocities in this study without losing any flow structure. The main advantage of selecting this angle-window over the smaller one is that the number of samples in this window is much higher so that the statistical uncertainties in the values of mean and rms velocities are minimised.

The mean flow variation in successive chambers is presented in Fig. 5 for a speed of 1000 rpm, at two radial locations, namely r=42 mm, which is near the rotor shaft, and at 62 mm, which is near the rotor tip. In general, a similar mean flow variation can be seen in all the working chambers except for chamber number 1 where the mean flow is substantially different from that in the other four chambers especially in the region close to the leading edge. This may be due to some defect in the rotor boundary of that flow chamber since it was observed at all the measuring points and operating conditions that were investigated. It will be investigated once the compressor is dismantled. The mean flow structures in chambers 2 to 5 are remarkably similar with a maximum deviation of 10% close to the leading edges of the rotor's lobes. This similarity will allow the results of these working chambers to be combined to produce a single curve to present the mean flow variation inside the working chamber from the trailing edge to the leading edge. It should be noted that the angular flow passage at r=42 mm, which is well inside the working chamber, is around 11°. This is five times smaller than that at r=62 mm, near the tip, which is around 55°, and is due to changes in the rotor profile geometry.

Similar results to that of Fig. 5 are presented in Fig. 6 but for turbulence velocity fluctuation. The same conclusion can be drawn from the results except that the difference between the rms velocity profile of working chamber number 1 and working chambers 2 to 5 is not as large as those observed in the mean flow variation of Fig. 5. Again, the same conclusions were obtained at all radial locations and operating conditions as, for example, at a speed of 750 rpm.

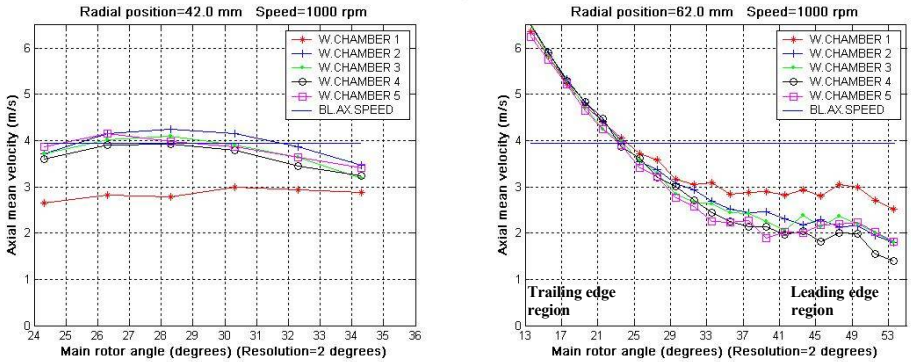

(a) (b)

Figure 5 Working chamber to chamber angular variation of axial mean velocity at two radial positions of r=42 and 62 mm and at a rotational speed of 1000 rpm.

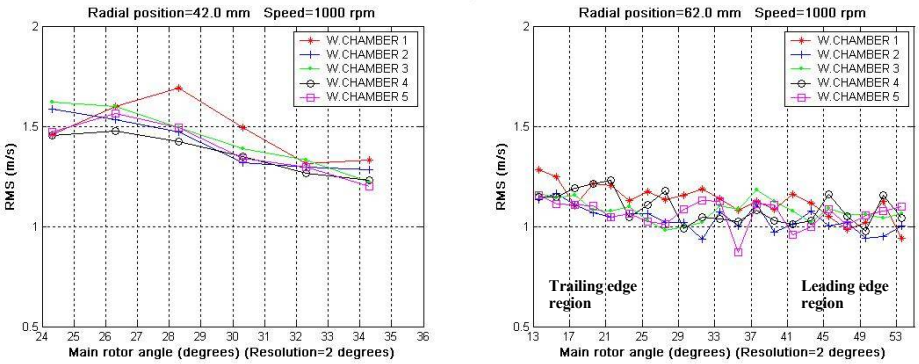

(a) (b)

Figure 6 Working chamber to chamber angular variation of axial rms velocity at two radial positions of r=42 and 62 mm and at a rotational speed of 1000 rpm.

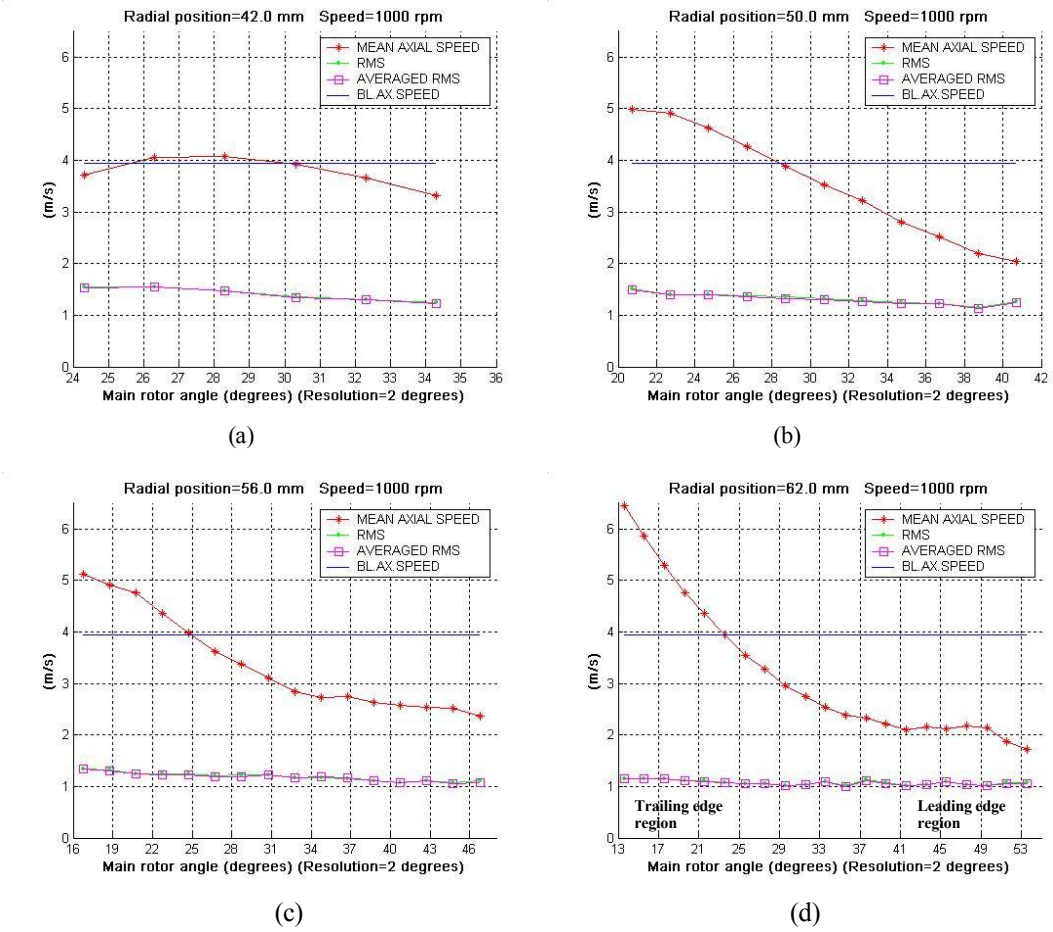

Figure 7 Angular variations of axial mean and rms velocities across the working chamber at different radial positions and for a rotational speed of 1000 rpm.

The turbulence velocity fluctuation at all radial locations shows generally similar trends, with the maximum value at the trailing edge reducing gradually towards the leading edge. But the turbulence levels at different radial locations are markedly different so that at the bottom of the chamber the root mean square velocities are higher and, as the radius is increased, they are reduced with the minimum values near the tip of the blades at r=62 mm. This suggests that the flow mixing is much better deep inside the working chamber than at the near tip region. To show these differences more clearly the mean and rms velocities at different radial locations are plotted in the same graph and are presented in Fig. 8. Figure 8(a) presents a comparison between the mean axial velocity profiles at different radial locations within the working chamber. A peaked profile can be seen at the lowest measured radius, r=42 mm, near the bottom of the chamber. As the flow passage expands at the larger radii the velocity profiles change with a shift of the peak value towards the trailing edge, so that the velocity profile near the tip, where r=62 mm, has a maximum at the trailing edge and reduces rapidly towards the leading edge where it become almost uniform. This flow transformation with radius suggests that strong transverse radial and circumferential flows exist in the working chamber. A comparison between the turbulence velocity fluctuations at different radial position, shown in Fig 8(b), clearly shows a reduction in turbulence level with angular position at all radii. It is also evident that the level of turbulence is substantially higher at the lower radii near the trailing edge of the rotor, with a maximum difference of up to 40% between r=42 mm and r=62 mm. These differences reduce with angular position so that near the leading edge they become almost identical.

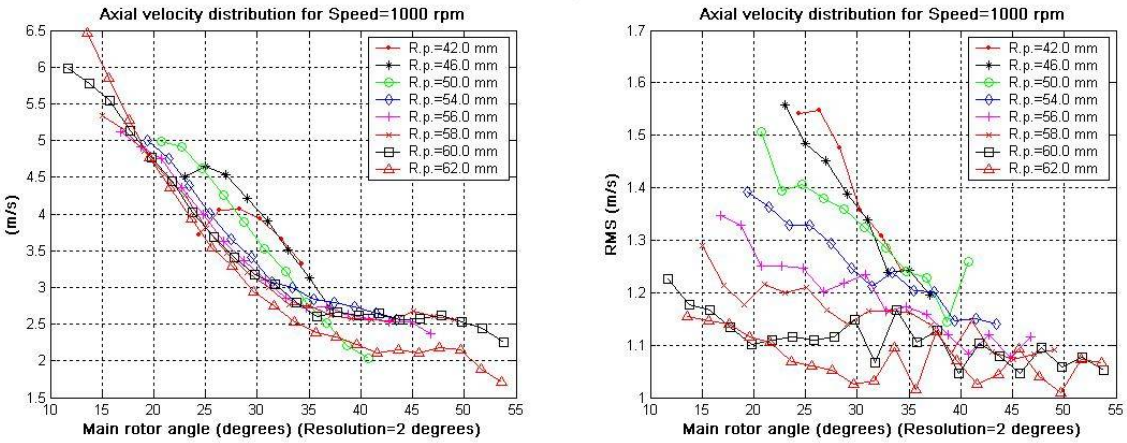

(a) (b)

Figure 8 Axial mean and turbulent flow development across the working chamber at different radial positions of r=60 mm and for a rotational speed of 1000 rpm.

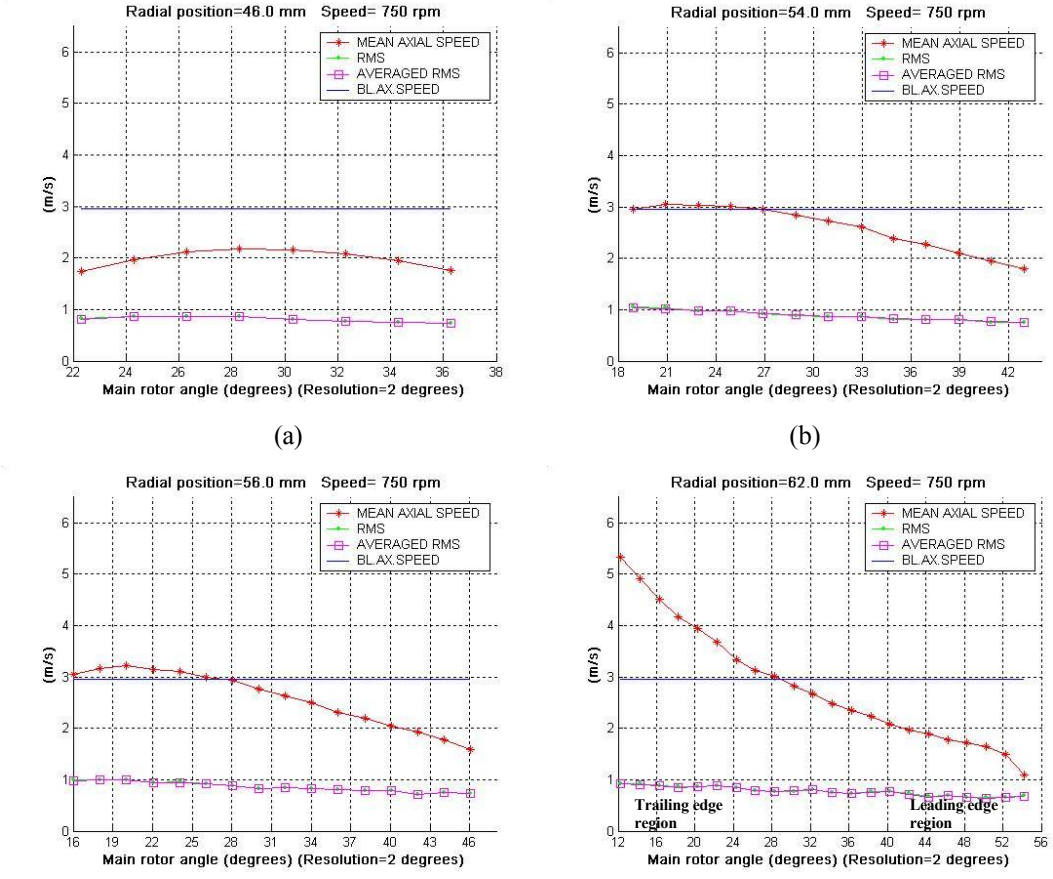

(a) (b)

(c) (d)

Figure 9 Angular variations of axial mean and rms velocities across the working chamber at different radial positions and for a rotational speed of 750 rpm.

Limited measurements at a rotational speed of 750 rpm are presented in Fig 9, similarly to those of Fig. 7 for 1000 rpm. The results show the same trend as those for 1000 rpm both for the mean and rms velocities. The maximum mean axial velocity at the trailing edge was 5.3 m/s, or $1.75V_p$.

4. FUTURE PROGRAMME

Flow characteristics at suction, discharge and within the rotors of compressor will be obtained as a function of rotational speed, up to 3000 rpm, using the 2-D LDV system; point measurements will include the phase-averaged mean and rms velocity components together with the turbulent cross-correlation.

The 2-D instantaneous flow characteristics will be obtained at the inlet and outlet sections for different rotational speeds using the micro PIV system. An attempt will also be made to make similar measurements in the interlobe region; the uncertainty of obtaining measurements in this region stems from the difficulty of installing two orthogonal transparent windows for the transmitting and collecting optics in this region of the compressor.

The measured data will be continually compared with internal flow predictions obtained from the in-house CFD model which will thus be validated over a range of operating conditions.

5. CONCLUSIONS

Axial mean flow and turbulence were successfully measured inside a screw compressor working chamber with high spatial and temporal resolution using laser Doppler velocimetry (LDV) at operating rotor speeds of 750 and 1000 rpm.

A temporal resolution of 0.1° of the rotor angle could be achieved, but the results of axial mean and rms velocity showed that the flow structure remained unchanged for an angular resolution of up to 2°. Axial mean and turbulent flow variation was found to be very similar in successive working chambers within the male rotor, with maximum differences of 10% near the leading edge of the blade. The results showed that, in general, the mean axial flow within the working chamber decreased from the trailing edge to the leading edge by up to 1.64 and 1.75 times for rotational speeds of 750 and 1000 rpm, respectively. A similar trend was found in rms velocity fluctuations with maximum levels at the trailing edge reducing to a minimum at the leading edge and with the turbulence level in the bottom of chamber up to 40% higher than that near the rotor tip.

It is hoped that this will assist in the development of a reliable CFD model of flow and pressure distribution within twin screw machines, which can be used as a tool to further improve their design both as compressors and expanders.

6. ACKNOWLEDGEMENTS

Financial support from EPSRC (under Research Grant EP/C541456/1), Trane, Lotus and Gardner Denver is gratefully acknowledged. The authors would like to thank Michael Smith, Jim Ford and Grant Clow for valuable technical support during the course of this work.

REFERENCES

1. Kampanis N, Arcoumanis C, Kato R, Kometani S, Flow, combustion and emissions in a five-valve research gasoline engine. *SAE Paper* 2001-013556.

2. Y. Yan Y, Gashi S, Nouri J M, Lockett R D and Arcoumanis C, Investigation of spray characteristics in a spray guided DISI engine using PLIF and LDV, *2nd Int. Conference on Optical Diagnostics, ICOLD,* London, September 2005.

3. Liu, C. H., Nouri, J.M., Vafidis, C. and Whitelaw, J.H. Experimental study of flow in a centrifugal pump, 5th International Symposium on Applications of Laser Techniques to Fluid Mechanics, July 1990.

4. Arcoumanis, C., Martinez-Botas, R., Nouri, J. M. and Su, C. C. Performance and exit flow characteristics of mixed flow turbines. International Journal of Rotating Machinery, **3**, No. 4, *pp*. 277-293, 1997.

5. Arcoumanis, C., Martinez-Botas, R., Nouri, J. M. and Su, C. C. Inlet and exit flow characteristics of mixed flow turbines. ASME, International gas Turbine and Aeroengine Congress and Exhibition, Paper 98-GT-495, June 2-5, 1998, Stockholm.

6. Zaidi, S. H. and Elder, R. L., "Investigation of flow in a radial turbine using laser anemometry", ASME, Int. Gas Turbine and Aeroengine Congress and Exhibition*,* Cincinnati, Ohio, May 24-27, 1993, ASME paper 93-GT-55.

7. Hockey R M, Nouri J M, Turbulent flow in a baffled vessel strirred by a 60 pitched blade impeller. *Chem. Eng. Science,* vol. 51, pp. 4405-4421, 1996.

8. Stosic N, On gearing of helical screw compressor rotors, Proc IMechE, v212, Part C pp587-594, 1998

9. Kovacevic A, Stosic N, Smith I. K. The CFD Analysis of a Screw Compressor Suction, International Compressor Engineering Conference, Purdue, 2000, p. 909

10. Kovacevic A, Stosic N, Smith I. K. Grid Aspects of Screw Compressor Flow Calculations, Proceedings of the ASME Congress 2000, Advanced Energy Systems Division, Vol. 40, 83

11. Kovacevic A, Stosic N, Smith I K, Analysis of Screw Compressor by Means of Three-Dimensional Numerical Modelling, International Conference on Compressor and their Systems, IMechE Conference, Transactions 2001-7, London, 2001, p.23-32

12. Kovacevic A, Stosic N, Smith I. K**,** Numerical Simulation of Fluid Flow and Solid Structure in Screw Compressors, ASME Congress 2002, Advanced Energy Systems Division, New Orleans, November 2002

13. Kovacevic A, Stosic N, Smith I. K**,** Numerical Study of the Solid Structure and Fluid Flow Interaction in Screw Compressors, Accepted for publication in International Journal of Computer Applications in Technology, 2003

14. Kovacevic A, Stosic N, Smith I. K**,** Three Dimensional Numerical Analysis of Screw Compressor Performance, Accepted for publication in Journal of Computational Methods in Sciences and Engineering for 2003

15. Kovacevic, A.; Stosic, N.; Smith, I.K.; "CFD Analysis of Screw Compressor Performance ", In: "Advances of CFD in Fluid Machinery Design" edited by Elder, R.L, Tourlidakis, A, Yates M.K, Professional Engineering Publishing, London, 2002

16. Arcoumanis, C., French, B. and Nouri, J. M. Steady intake flow characteristics through a diesel four-valve cylinder head. 8th International Symposium on Applications of Laser Techniques to Fluid Mechanics, Lisbon, July 8-11, 1996.

17. Distelhoff, M. F. W., Marquis, A. J., Nouri, J. M. and Whitelaw, J. H. Power and concentration measurements in a stirred tank with different impellers. The Canadian Journal of Chemical Engineering, 75, *pp.* 641-652, 1997

18. Nouri, J. M., Brehm, C. and Whitelaw, J. H. The spray from a gasoline direct injection engine. ILASS99 Symposium, 5-7 July, 1999, Toulouse, France.

19. Nouri, J. M. and Whitelaw, J. H. Spray characteristics of a GDI injector with short duration of injection. Experiments in Fluids, 2001.

20. Zaidi, S. H. and Elder, R. L., "Investigation of flow in a radial turbine using laser anemometry", ASME, Int. Gas Turbine and Aeroengine Congress and Exhibition*,* Cincinnati, Ohio, May 24-27, 1993, ASME paper 93-GT-55.

21.